Journal of RADIATION INDUSTRY

Vol. 19, No. 3, pp. 257-265, 2025
https://doi.org/10.23042/radin.2025.19.3.257

Original article

Formulation of Curcumin Nanoemulsions via Chitosan Coating and Gamma Irradiation

Do-Yeong Kim[1] and Jae-Kyung Kim[2,*]

[1]Division of Food and Nutrition, Chonnam National University, Gwangju 61186, Republic of Korea
[2]Advanced Radiation Technology Institute, Korea Atomic Energy Research Institute, Jeongeup 56212, Republic of Korea

ABSTRACT Curcumin, a bioactive compound with extensive therapeutic potential, suffers from poor water solubility and low bioavailability, limiting its application in functional food and pharmaceutical formulations. In this study, a novel curcumin-loaded nanoemulsion (NE) system coated with low molecular weight chitosan (LMWC) was developed and stabilized via gamma irradiation. The nanoemulsions were prepared using medium-chain triglyceride (MCT) oil, lecithin, and tween 80, and then surface-modified with chitosan to enhance structural stability. Gamma irradiation (0-10 kGy) was applied to investigate its effect on droplet size, polydispersity index (PDI), and color values. Among the formulations tested, LCNEs prepared with 0.3-0.5% LMWC and irradiated at 5-10 kGy exhibited the smallest particle sizes (<300 nm) and narrow size distribution (PDI<0.3), suggesting enhanced emulsification and interfacial compaction. Gamma irradiation resulted in increased lightness (L*) and redness (a*), but decreased yellowness (b*), especially in samples containing higher LMWC concentrations. Storage stability tests revealed that gamma-irradiated LCNEs maintained droplet integrity over 15 days, while pH stability evaluation demonstrated improved resistance to aggregation at neutral pH. Conversely, samples stored under acidic conditions (pH 3.0 and 5.0) showed increased droplet size and PDI over time, indicating instability due to reduced electrostatic repulsion. These findings highlight the synergistic effect of chitosan coating and gamma irradiation in producing stable, small-sized nanoemulsions suitable for delivering hydrophobic nutraceuticals like curcumin in food and pharmaceutical systems.

Key words: Curcumin, Chitosan, Emulsion, Gamma-irradiation

1. Introduction

Nutraceuticals, known for their potential to support human health and prevent chronic diseases, are gaining increasing attention with the rising demand for functional foods and preventive healthcare [1]. Among them, curcumin, the principal bioactive compound extracted from *Curcuma longa* (turmeric), has been extensively studied for its diverse pharmacological activities, including antioxidant, anti-inflammatory, anticancer, and antimicrobial properties [2-4]. With thousands of years of traditional usage and classification as "generally recognized as safe (GRAS)" by both the Food and Drug Administration (FDA) and World Health Organization (WHO), curcumin has a strong safety profile and historical significance [5,6]. However, despite these benefits, curcumin's application in food, pharmaceutical, and cosmetic industries remain limited due to its low aqueous solubility and instability under various environmental conditions such as heat, light, and pH variations [7,8]. Its strong inter- and intramolecular hydrogen bonding restricts dissolution, and rapid metabolism and poor absorption contribute to its notably low bioavailability *in vivo* [9,10]. Therefore, effective delivery systems are necessary to enhance its solubility, protect it from degradation, and improve bioaccessibility.

Nanoemulsions (NEs), especially oil-in-water (o/w) systems, have emerged as promising delivery vehicles for lipophilic nutraceuticals like curcumin due to their ability to improve solubility, protect active ingredients, and enable controlled release [1,11]. With droplet sizes typically below 200 nm, NEs provide enhanced stability, fast absorption, and increased surface area for interaction, which translates to better bioavailability and therapeutic efficacy [12,13]. In particular, medium-chain triglyceride (MCT) oils, coupled with food-grade surfactants

ISSN 1976-2402 **http://www.ksri.kr/**

Copyright© 2025 by Korean Society of Radiation Industry

***Corresponding author:** Jae-Kyung Kim
Tel: +82-63-570-3219, Fax: +82-63-570-3207, E-mail: jkim@kaeri.re.kr

Received 18 July 2025 **Revised** 21 July 2025 **Accepted** 30 July 2025

like Tween 80 and lecithin, have been used to prepare stable curcumin nanoemulsions [14,15]. Despite the improved performance of nanoemulsions, their physical stability remains a concern under external stresses such as thermal processing, light exposure, and ionic fluctuations, which are common in food manufacturing and storage [16,17]. To address these issues, surface modification using biopolymers has been employed to form multilayered or coated emulsions that offer enhanced protection against environmental degradation and controlled delivery of the payload [18,19].

Chitosan, a natural cationic polysaccharide derived from chitin, has been widely utilized as a coating material due to its biocompatibility, mucoadhesiveness, and antimicrobial properties [8,20]. Chitosan coating not only improves the physical stability of emulsions by providing electrostatic and steric repulsion but also modulates the release profile of bioactives in the gastrointestinal tract [21,22]. Furthermore, gamma irradiation—a non-thermal sterilization method—has been explored for food and pharmaceutical applications, offering the ability to enhance microbial safety without causing thermal damage to heat-sensitive compounds like curcumin. However, the interaction between chitosan-coated nanoemulsions and gamma irradiation, especially concerning structural integrity, curcumin retention, and functional performance, has not been thoroughly investigated.

In this study, we aimed to develop a gamma-irradiated curcumin-loaded nanoemulsion system coated with chitosan and evaluate its physicochemical properties, stability, and potential application in functional foods. Specifically, the effects of gamma irradiation and chitosan coating on droplet size, zeta potential, and polydispersity index (PDI) were assessed.

2. Materials and Methods

2.1. Materials

Curcumin (≥95% pure) was purchased from Acros Orangnics (NJ, USA). Medium-chain triglycerides (MCT) and soy lecithin were obtained from Piping Rock (Ronkonkoma, NY, USA) and Junsei Chemical Co. (Tokyo, Japan), respectively. Tween 80 (polysorbate 80) was purchased from Samchun Chemical Co. (Pyeongtaek, Korea). Chitosan with different molecular weights were purchased from Sigma-Aldrich (MO, USA), including a high molecular weight chitosan (MW 190,000-310,000 Da), a medium molecular weight chitosan (MW 30,000 Da), and a low molecular weight chitosan (MW 3,000 Da). Other chemicals and reagents used in this study were of analytical grade.

2.2. Preparation of chitosan-coated nanoemulsion (CNE)

Curcumin-loaded nanoemulsion (NE) was prepared using a two-step emulsification process involving high-speed homogenization and ultrasonication. Initially, 70 mg of curcumin was dissolved in 10 mL of MCT oil under mild heating with overnight stirring to ensure complete solubilization. After filtering through a 0.45 μm syringe filter to remove any undissolved particles, the MCT oil containing curcumin was mixed with soy lecithin, Tween 80, and distilled water at a weight ratio of 10 : 6 : 4 : 80 (MCT oil : lecithin:Tween 80 : water). The mixture was first stirred at 200 rpm to homogenize the components. Then, the pre-emulsion was subjected to high-speed homogenization at 16,000 rpm for 5 min using a high-speed homogenizer (Ultra-Turrax T25, IKA, Germany). The resulting coarse emulsion was further processed by ultrasonication at a power of 150 W for 20 min in an ice bath to produce a stable nanoemulsion.

Chitosan-coated nanoemulsion (CNE) was prepared by surface modification of the NE with chitosan. Chitosan powder of varying molecular weights (low, medium, and high) was dissolved in 2% (v/v) acetic acid at a concentration of 0.3% (w/v) and stirred overnight at room temperature to ensure complete dissolution. The solution was filtered using qualitative filter paper to remove any undissolved particles. Equal volumes (1 : 1, v/v) of NE and chitosan solution were mixed under magnetic stirring overnight to allow sufficient interaction between the negatively charged nanoemulsion droplets and the positively charged chitosan molecules. The resulting mixture was then subjected to ultrasonication at 150 W for 10 min in an ice bath to reduce droplet size and prevent bridging flocculation that can occur due to chitosan chain entanglement. Following sonication, the CNE samples were exposed to gamma-irradiation at varying doses of 0, 1, 5, and 10 kGy using a cobalt-60 source. Based on the characterization results of CNEs prepared using chitosan with different molecular weights, low molecular weight chitosan (LMWC) was found to be the most suitable for CNE fabrication. Therefore, subsequent experiments were conducted using LMWC at varying concentrations of 0, 0.1, 0.3, and 0.5% to prepare CNEs (LCNE) and evaluate their physicochemical properties and stability.

2.3. Characterization of CNE

2.3.1. Particle size and zeta potential

The particle size distribution, polydispersity index (PDI), and zeta potential of CNE were measured using dynamic light

scattering (DLS) on a Zetasizer Nano-ZS (Malvern Instruments Ltd., Worcestershire, UK). Samples were diluted fivefold with distilled water to minimize multiple scattering effects and analyzed at 25°C with a scattering angle of 90° and laser wavelength of 633 nm. Each measurement was performed in triplicate.

2.3.2. Color

The color attributes of the LCNE samples were evaluated using a colorimeter (CR-400 Chroma Meter; Minolta Co., Ltd., Osaka, Japan). The instrument was calibrated with a standard white plate (L*=96.94, a*=0.07, b*=2.33) prior to measurement. Color parameters were recorded based on the CIE Lab* color space, where L* represents lightness (ranging from 0 to 100), a* indicates the red-green axis (positive values indicate redness, negative values indicate greenness), and b* corresponds to the yellow-blue axis (positive values indicate yellowness, negative values indicate blueness). Each measurement was conducted in triplicate, and the mean values were reported.

2.4. Stability evaluation of CNE

2.4.1. Storage stability

The storage stability of NE and CNE was assessed by storing the samples in sealed glass vials at 25°C. Physicochemical properties including particle size, PDI, and zeta potential were monitored at predetermined time points (0, 7, and 15 days) using the same DLS protocol to evaluate changes during storage.

2.4.2. pH stability

To evaluate pH stability, 10 mL of each NE and CNE sample was adjusted to pH 3.0, 5.0, and 7.0 using HCl or NaOH solutions. After adjustment, the samples were stored at room temperature, and their particle size and PDI were measured at 0, 5, and 18 hours to assess the physical stability of the emulsions under various pH conditions.

2.5. Statistical analysis

All experiments were performed in triplicate, and the results were expressed as mean±standard deviation (SD). Statistical analyses were performed using one-way analysis of variance (ANOVA), followed by the post hoc Tukey's test ($p<0.05$) with SPSS software (version 20.0; SPSS Inc., Chicago, IL, USA).

3. Results and Discussion

3.1. Preparation of chitosan-coated nanoemulsion (CNE)

The characterization results of CNEs prepared with different molecular weight chitosans are summarized in Table 1. In this study, curcumin-loaded chitosan-coated nanoemulsions (CNEs) were fabricated using chitosan of varying molecular weights (low, medium, and high) and subjected to different gamma irradiation doses (0, 1, 5, and 10 kGy). The nanoemulsions were prepared using MCT oil as the lipid phase to dissolve curcumin and an ultrasonication method, following protocols similar to previous studies [23,24]. Tween 80 and lecithin were employed as surfactant and co-surfactant, respectively, to stabilize the nanoemulsion and provide negative surface charge. After coating the prepared nanoemulsions with chitosan (CNE), significant changes in particle size, polydispersity index (PDI), and zeta potential were observed. Particularly, nanoemulsions coated with low molecular weight chitosan (LMWC) without irradiation (0 kGy) showed a relatively large particle size of 860 nm, a moderate PDI of 0.359, and a nearly neutral zeta potential of −0.5 mV. However, as the gamma irradiation dose increased, the particle size of the LMWC-coated CNEs was notably reduced to 735 nm, 430 nm, and 296 nm at 1, 5, and 10 kGy, respectively. In contrast, nanoemulsions coated with medium (MMWC) and high molecular weight chitosan (HMWC) exhibited significantly larger initial particle sizes, with 1562 nm and 1034 nm, respectively, under non-irradiated conditions. While gamma irradiation also reduced the particle sizes in these groups, the smallest sizes achieved at 10 kGy were still comparatively high at 757 nm for MMWC and 671 nm for HMWC. Additionally, these samples showed higher PDI values than the LMWC-coated CNEs, indicating broader size distribution and reduced homogeneity. These findings are consistent with previous reports showing that chitosan with higher molecular weight tends to form thicker and less compact coating layers, resulting in increased particle size and heterogeneity [21,25]. Based on these results, LMWC was selected for further experiments, and CNEs were fabricated using different concentrations of low molecular weight chitosan. This formulation was considered optimal due to its smaller particle size, narrower distribution, and improved surface charge properties after gamma irradiation, which are critical for enhancing nanoemulsion stability, cellular uptake, and potential bioavailability [26,27]. Figure 1 presents a schematic illustration of CNE.

Table 1. Characterization of curcumin-loaded chitosan-coated nanoemulsions (0.3% CNE) using LMWC, MMWC, and HMWC under different gamma irradiation doses

Chitosan 0.3%	Dose (kGy)	Particle size (d,nm)	Polydispersity index (PDI)	Zeta-potential (mV)
LMWC	0	$860.7\pm35.2^{a,y}$	$0.359\pm0.005^{a,y}$	-0.5
	1	$735.2\pm49.7^{b,y}$	$0.331\pm0.001^{b,y}$	3.2
	5	$430.1\pm6.9^{c,y}$	$0.325\pm0.013^{b,y}$	0.8
	10	$296.9\pm4.7^{d,y}$	$0.330\pm0.010^{b,y}$	-1.5
MMWC	0	$1562.3\pm273.8^{a,x}$	$0.633\pm0.106^{a,x}$	-0.3
	1	$1401.0\pm256.6^{ab,x}$	$0.571\pm0.087^{ab,x}$	3.0
	5	$1157.6\pm113.7^{ab,x}$	$0.475\pm0.041^{ab,x}$	-0.8
	10	$757.7\pm133.6^{b,x}$	$0.326\pm0.038^{b,x}$	-12.8
HMWC	0	$1034.1\pm182.9^{ab,y}$	$0.436\pm0.062^{a,y}$	-4.5
	1	$1284.7\pm68.3^{a,x}$	$0.525\pm0.026^{a,x}$	-9.4
	5	$987.3\pm159.1^{ab,x}$	$0.415\pm0.067^{ab,x}$	-2.8
	10	$671.9\pm132.6^{b,x}$	$0.291\pm0.045^{b,x}$	0.8

Values are expressed as mean ± standard deviation. Different superscripts (a-d) within the same chitosan molecular weight group indicate significant differences among gamma irradiation doses ($p<0.05$) according to Tukey's HSD test. Different letters (x, y) within the same irradiation dose indicate significant differences among chitosan molecular weights.

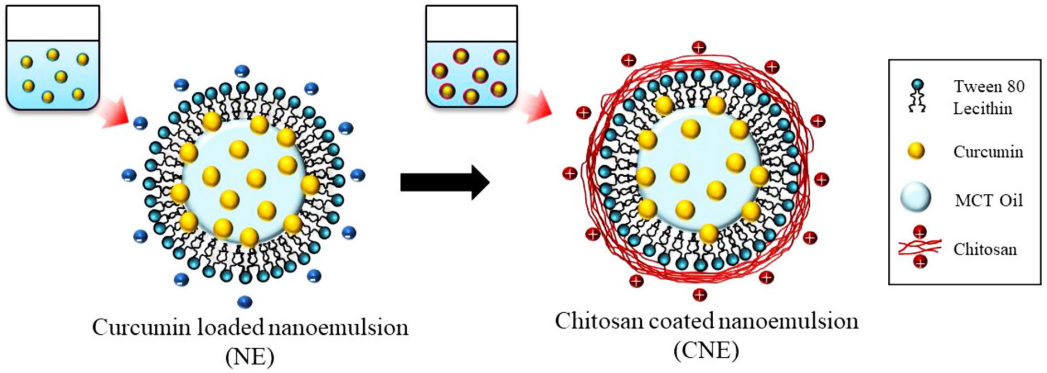

Fig. 1. Schematic illustration of CNE

3.2. Characterization of LMWC-coated nanoemulsion (LCNE)

As shown in Fig. 2, the mean droplet size of LCNEs increased with increasing LMWC concentration, in line with prior observations that chitosan adsorption onto the surface of emulsion droplets leads to an increase in size due to polymer layering and charge repulsion [28]. However, at 0.5% chitosan, both the particle size and PDI values were slightly reduced compared to 0.3%, suggesting a denser and more compact chitosan layer possibly due to self-rearrangement during emulsification or stronger interfacial interactions.

Upon gamma irradiation, a notable reduction in particle size was observed in LCNEs with 0.3% and 0.5% LMWC. For example, in the 0.3% LMWC group, the droplet size decreased from 729.9 nm (0 kGy) to 375.8 nm (10 kGy), while in the 0.5% group, it decreased from 480.0 nm to 231.4 nm with increasing irradiation dose. This size reduction may be attributed to radiation-induced breakdown or reorganization of the chitosan coating, enhancing emulsification efficiency by improving droplet surface coverage and reducing interfacial tension. Notably, no significant changes in size or PDI were observed for emulsions containing 0% and 0.1% LMWC, indicating that gamma irradiation effects are more pronounced in systems with a higher chitosan content. These findings align with earlier reports where polymer-coated nanoemulsions exhibited enhanced compactness or droplet fragmentation upon thermal or ionic treatments [29,30]. The consistently low PDI (<0.3) values across all treatments suggest a relatively uniform droplet distri-

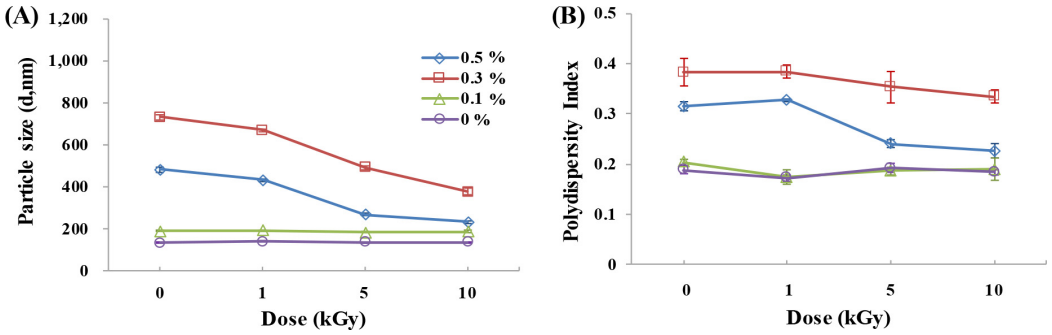

Fig. 2. Particle size (A) and polydispersity index (B) of LMWC-coated nanoemulsion (LCNE)

Table 2. Color values of curcumin-loaded LMWC-coated nanoemulsion (LCNE, 0-0.5%) under different gamma irradiation doses

LMWC concentration (%)	Dose (kGy)	L*	a*	b*
0	0	55.37±0.01^{d,z}	-19.08±0.03^{b,z}	55.25±0.02^{a,z}
	1	56.26±0.01^{c,z}	-21.24±0.02^{c,z}	53.71±0.02^{b,z}
	5	57.98±0.01^{b,z}	-22.38±0.02^{d,z}	31.17±0.01^{c,z}
	10	59.53±0.02^{a,z}	-9.12±0.01^{a,z}	-7.71±0.01^{d,z}
0.1	0	71.08±0.02^{d,x}	-15.93±0.01^{b,x}	66.22±0.01^{a,x}
	1	72.63±0.01^{c,w}	-17.51±0.03^{c,x}	64.88±0.03^{b,x}
	5	74.60±0.07^{b,x}	-18.17±0.01^{d,x}	40.52±0.12^{c,x}
	10	75.44±0.07^{a,x}	-6.88±0.01^{a,x}	0.66±0.07^{d,y}
0.3	0	71.92±0.02^{d,w}	-11.81±0.02^{b,w}	75.14±0.03^{a,w}
	1	72.22±0.05^{c,x}	-13.69±0.01^{c,w}	72.85±0.07^{b,w}
	5	74.57±0.08^{b,x}	-14.60±0.01^{d,w}	42.78±0.10^{c,w}
	10	76.08±0.03^{a,w}	-5.44±0.01^{a,w}	6.52±0.03^{d,w}
0.5	0	66.38±0.07^{d,y}	-17.43±0.06^{b,y}	62.32±0.15^{b,y}
	1	68.60±0.11^{c,y}	-18.38±0.04^{c,y}	62.65±0.18^{a,y}
	5	71.05±0.05^{b,y}	-18.44±0.01^{c,y}	37.74±0.10^{c,y}
	10	72.02±0.02^{a,y}	-8.35±0.01^{a,y}	0.97±0.01^{d,x}

Values are expressed as mean ± standard deviation. Different superscripts (a–d) within the same chitosan concentration group indicate significant differences among gamma irradiation doses ($p < 0.05$) according to Tukey's HSD test. Different letters (w-z) within the same irradiation dose indicate significant differences among chitosan concentration.

bution and high dispersion stability of the LCNEs.

Table 2 summarizes the results of colorimetric analysis of the LCNE samples. Colorimetric analysis revealed significant changes in the visual appearance of LCNEs depending on LMWC concentration and irradiation dose. In general, gamma irradiation resulted in increased lightness (L*) and redness (a*), but decreased yellowness (b*), especially in samples containing higher LMWC concentrations. This may be due to oxidative or structural changes in curcumin and chitosan upon exposure to gamma radiation, altering light scattering and absorption properties of the emulsions. As LMWC concentration increased, all color parameters (L*, a*, and b*) tended to increase, indicating that the chitosan coating enhanced emulsion turbidity and chromaticity, possibly due to increased interfacial thickness and improved light scattering [31]. However, at 0.5% chitosan, a reversal trend was observed where L*, a*, and b* values slightly decreased compared to those of the 0.3% group. This unexpected behavior might be attributed to excessive chitosan aggregation or gelation at higher concentrations, which could hinder uniform coating and light interaction, leading to reduced optical clarity and color intensity. These observations are consistent with previous studies reporting that emulsion encapsulation and interfacial structure significantly impact optical properties such as brightness and color saturation [32,33]. Moreover, gamma

irradiation may influence the oxidation of curcumin or detachment of surface chitosan, further affecting the emulsion's visual characteristics.

3.3. Stability of CNE

The storage stability of low molecular weight chitosan-coated nanoemulsions (LCNEs) was assessed by measuring changes in particle size and PDI over a 15-day period at room temperature. As shown in Fig. 3, the non-irradiated LCNE sample (0 kGy) initially exhibited a particle size of 860.7 nm, which slightly increased to 922.3 nm on day 7, then decreased significantly to 709.5 nm by day 15. In parallel, the PDI value showed a steady decline from 0.359 to 0.310, indicating an improvement in droplet uniformity over the storage period. Interestingly, LCNE samples treated with gamma irradiation displayed a consistent trend of size reduction during storage. For example, the particle size of the 1 kGy-treated sample decreased from 735.2 nm on day 0 to 526.5 nm on day 15, while the 5 and 10 kGy samples decreased from 430.1 to 336.4 nm, and from 296.9 to 295.2 nm, respectively. This progressive reduction in droplet size may be attributed to the rearrangement of chitosan chains into a more thermodynamically stable configuration at the droplet interface, or to the improved emulsification efficiency and surface coverage induced by gamma irradiation. Moreover, the sampling method—specifically, drawing emulsions from the bottom of the storage container—might have contributed to the observed decrease in particle size, as larger droplets may have migrated upwards due to gravitational separation. Similar effects have been reported in other studies where sample stratification during storage influenced droplet size measurements [29,30]. Despite these changes, PDI values for all samples remained below 0.4 throughout the storage period, confirming the high dispersion stability of LCNEs. These findings suggest that LCNEs, especially those treated with moderate to high doses of gamma irradiation, exhibit excellent short-term storage stability due to combined steric stabilization from chitosan and enhanced droplet compaction facilitated by irradiation.

The pH stability of LCNEs was evaluated by measuring particle size and PDI over time (0, 5, and 18 hours) at three different pH levels (3.0, 5.0, and 7.0), using varying doses of gamma irradiation (0, 1, 5, and 10 kGy) during formulation (Table 3). The results demonstrated that both pH and irradiation dose significantly influenced the initial and time-dependent colloidal stability of the LCNEs. At 0 hours, non-irradiated samples exhibited a clear dependence of particle size on pH. The particle sizes were 1195.1 nm at pH 3.0, 1185.6 nm at pH 5.0, and markedly smaller at 309.8 nm at pH 7.0. After 18 hours, the particle sizes at pH 3.0 and 5.0 increased substantially to 2678.6 and 1892.9 nm, respectively, indicating significant instability and possible droplet aggregation. In contrast, the particle size at pH 7.0 slightly decreased to 278.6 nm, suggesting improved structural integrity under near-neutral conditions. Gamma irradiation played a stabilizing role, as samples prepared at higher doses (particularly 5 and 10 kGy) showed a consistent reduction in initial particle size across all pH conditions. For instance, at pH 3.0 and 5.0, the 0-hour particle sizes decreased with increasing irradiation dose, supporting the hypothesis that irradiation improves emulsification efficiency and facilitates more compact interfacial chitosan organization. A similar trend was observed for PDI values, which generally decreased with higher irradiation doses, indicating enhanced uniformity, except in the pH 5.0 condition where PDI did not follow a clear trend.

During the 18-hour storage, particle size and PDI values increased at both pH 3.0 and 5.0, likely due to protonation of

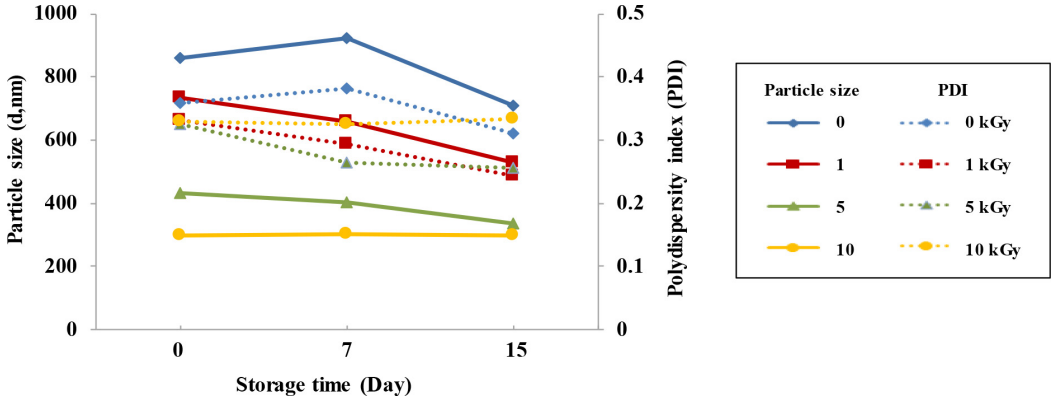

Fig. 3. Storage stability of LMWC-coated nanoemulsion (LCNE)

Table 3. pH stability of LMWC-coated nanoemulsion (LCNE)

Time (hour)	Does (kGy)	pH 3		pH 5		pH7	
		Particle size (d, nm)	Polydispersity index (PDI)	Particle size (d, nm)	Polydispersity index (PDI)	Particle size (d, nm)	Polydispersity index (PDI)
0	0	1195.1±669.2^{a,x}	0.359±0.161^{a,x}	1185.6±166.1^{a,x}	0.409±0.072^{a,x}	309.8±2.5^{a,x}	0.307±0.004^{a,x}
	1	1465.0±568.5^{a,x}	0.108±0.569^{a,x}	1215.8±366.5^{a,xy}	0.331±0.286^{a,x}	312.0±44.8^{a,y}	0.283±0.047^{ab,x}
	5	1166.2±163.9^{a,x}	0.451±0.021^{a,x}	697.9±37.7^{a,y}	0.423±0.040^{a,x}	197.1±2.8^{b,z}	0.288±0.008^{ab,y}
	10	860.3±203.1^{a,x}	0.276±0.256^{a,x}	751.7±130.7^{a,x}	0.415±0.021^{a,x}	185.4±3.9^{b,y}	0.244±0.015^{b,x}
5	0	2191.3±165.1^{a,x}	0.491±0.054^{a,x}	1582.1±180.6^{a,y}	0.428±0.035^{a,x}	389.9±21.5^{a,z}	0.252±0.013^{a,y}
	1	2502.5±362.8^{a,x}	0.520±0.146^{a,xy}	1914.1±363.2^{a,x}	0.533±0.110^{a,x}	368.3±27.2^{a,y}	0.261±0.020^{a,y}
	5	1526.3±206.2^{b,x}	0.471±0.070^{a,x}	589.6±47.5^{b,y}	0.429±0.022^{a,x}	213.2±3.9^{b,z}	0.266±0.028^{a,y}
	10	1226.2±200.4^{b,x}	0.510±0.033^{a,x}	870.8±65.2^{b,y}	0.459±0.022^{a,x}	378.5±4.4^{b,z}	0.527±0.006^{a,y}
18	0	2678.6±373.9^{b,x}	0.569±0.159^{a,x}	1892.9±179.9^{a,y}	0.482±0.073^{a,x}	278.6±51.6^{b,z}	0.188±0.024^{b,y}
	1	4543.1±342.7^{a,x}	0.608±0.519^{a,x}	1930.1±39.1^{a,y}	0.500±0.023^{a,x}	403.8±15.6^{a,z}	0.241±0.005^{a,x}
	5	3785.7±539.4^{a,x}	0.884±0.153^{a,x}	560.6±59.5^{c,y}	0.313±0.011^{b,y}	214.9±12.0^{b,y}	0.266±0.024^{a,y}
	10	1650.4±279.4^{b,x}	0.600±0.080^{a,x}	1040.3±187.4^{b,y}	0.471±0.020^{a,y}	216.4±3.8^{b,z}	0.278±0.007^{a,z}

chitosan's amino groups, which reduces electrostatic repulsion and promotes aggregation or bridging flocculation under acidic conditions. These results align with previous findings that chitosan-coated emulsions exhibit instability at low pH due to reduced surface charge and weakened interfacial stabilization [34,35]. Conversely, at pH 7.0, both particle size and PDI decreased over time, indicating that the LCNEs maintained or even improved their stability under neutral conditions. This may be attributed to reduced electrostatic interaction with surrounding media and potential rearrangement of chitosan at the interface, forming a more thermodynamically stable structure.

Overall, the pH 7.0 environment provided the most favorable conditions for LCNE stability, particularly in conjunction with gamma irradiation, which enhanced initial particle uniformity and long-term resistance to aggregation. These findings suggest that both pH and irradiation dose must be carefully considered to optimize the colloidal and structural stability of LCNEs for food and pharmaceutical applications.

4. Conclusions

This study demonstrated the successful fabrication LCNEs and stabilized by gamma irradiation. The application of LMWC significantly improved the physical stability of the nanoemulsions, while gamma irradiation further enhanced emulsification efficiency by reducing droplet size and improving homogeneity. pH stability assessments revealed that LCNEs are most stable at neutral pH, whereas acidic environments led to increased particle size and polydispersity, likely due to protonation of chitosan and reduced interfacial repulsion. Storage studies confirmed the long-term stability of irradiated LCNEs, with particle size and PDI values remaining consistent or even improving over time. Collectively, these findings indicate that the combination of chitosan surface modification and gamma irradiation is an effective strategy to overcome curcumin's solubility and stability limitations. This formulation approach offers promising potential for developing functional food and pharmaceutical delivery systems that require enhanced bioactive protection and controlled release.

Acknowledgment

This work was supported by the Korea Atomic Energy Research Institute (KAERI) Institutional Program (Project No. 523320-25).

References

1. McClements DJ. 2015. Nanoscale nutrient delivery systems for food applications: improving bioactive dispersibility, stability, and bioavailability. *J. Food Sci*. **80**:1602-1611. https://doi.org/10.1111/1750-3841.12919.
2. Aditya N, Shim M, Lee I, Lee Y, Im M-H and Ko S. 2013. Curcumin and genistein coloaded nanostructured lipid carriers: in vitro digestion and antiprostate cancer activity. *J. Agric. Food Chem.* **61**: 1878-1883. https://doi.org/10.1021/jf305143k.

3. Chainani-Wu N. 2003. Safety and anti-inflammatory activity of curcumin: a component of tumeric (*Curcuma longa*). *J. Altern. Complement. Med*. **9**:161-168. https://doi.org/10.1089/107555303321223035.
4. Oglah MK, Mustafa YF, Bashir MK, Jasim MH and Mustafa YF. 2020. Curcumin and its derivatives: A review of their biological activities. *Syst. Rev. Pharm.* **11**:472-481. http://dx.doi.org/10.5530/srp.2020.3.60.
5. Adsare SR and Annapure US. 2021. Microencapsulation of curcumin using coconut milk whey and Gum Arabic. *J. Food Eng*. **298**:110502. https://doi.org/10.1016/j.jfoodeng.2021.110502.
6. Cheng A, Hsu C, Lin J, Hsu M, Ho Y, Shen T, Ko J, Lin J, Lin B, Wu M and và Hsieh CY. 2001. Phase I clinical trial of curcumin, a chemopreventive agent, in patients with high-risk or pre-malignant lesions. *Anticancer Res*. **21**:2895-2900.
7. Heger M, van Golen RF, Broekgaarden M and Michel MC. 2014. The molecular basis for the pharmacokinetics and pharmacodynamics of curcumin and its metabolites in relation to cancer. *Pharmacol. Rev.* **66**:222-307. https://doi.org/10.1124/pr.110.004044.
8. Li J, Shin GH, Lee IW, Chen X and Park HJ. 2016. Soluble starch formulated nanocomposite increases water solubility and stability of curcumin. *Food Hydrocoll*. **56**:41-49. https://doi.org/10.1016/j.foodhyd.2015.11.024.
9. Dhillon N, Aggarwal BB, Newman RA, Wolff RA, Kunnumakkara AB, Abbruzzese JL, Ng CS, Badmaev V, and Kurzrock R. 2008. Phase II trial of curcumin in patients with advanced pancreatic cancer. *Clin. Cancer Res*. **14**:4491-4499. https://doi.org/10.1158/1078-0432.ccr-08-0024.
10. Li J, Lee IW, Shin GH, Chen X and Park HJ. 2015. Curcumin-Eudragit® E PO solid dispersion: a simple and potent method to solve the problems of curcumin. *Eur. J. Pharm. Biopharm*. **94**:322-332. https://doi.org/10.1016/j.ejpb.2015.06.002.
11. Berenji RH, Pezeshki A, Ghanbarzadeh B, Mohammadi M, Azar MT, Hamishehkar H, Azar FAN and Ghorbani M. 2021. Resveratrol entrapped food grade lipid nanocarriers as a potential antioxidant in a mayonnaise. *Food Biosci*. **41**:101041. https://doi.org/10.1016/j.fbio.2021.101041.
12. Setthacheewakul S, Mahattanadul S, Phadoongsombut N, Pichayakorn W and Wiwattanapatapee R. 2010. Development and evaluation of self-microemulsifying liquid and pellet formulations of curcumin, and absorption studies in rats. *Eur. J. Pharm. Biopharm*.**76**: 475-485. https://doi.org/10.1016/j.ejpb.2010.07.011
13. Tadros T, Izquierdo P, Esquena J and Solans C. 2004. Formation and stability of nano-emulsions. *Adv. Colloid Interface Sci*. **108**: 303-318. https://doi.org/10.1016/j.cis.2003.10.023.
14. Cao M, Liu C, Shi J, Ni F, Qi J, Shen Q, Huang M, Ren G, Tian S and Lin Q. 2021. Fabrication and characterization of oil-in-water Pickering emulsions stabilized by ZEIN-HTCC nanoparticles as a composite layer. *Food Res. Int*. **148**:110606. https://doi.org/10.1016/j.foodres.2021.110606.
15. Jiang T and Charcosset C. 2022. Premix membrane emulsification for the preparation of curcumin-loaded nanoemulsions. *J. Food Eng*. **316**:110836. https://doi.org/10.1016/j.jfoodeng.2021.110836.
16. Lee MH, Lee IY, Chun YG and Kim B-K. 2021. Formulation and characterization of β-caryophellene-loaded lipid nanocarriers with different carrier lipids for food processing applications. *LWT*. **149**: 111805. https://doi.org/10.1016/j.lwt.2021.111805.
17. Wu M-H, Yan HH, Chen Z-Q and He M. 2017. Effects of emulsifier type and environmental stress on the stability of curcumin emulsion. *J. Dispers. Sci. Technol.* **38**:1375-1380. https://doi.org/10.1080/01932691.2016.1227713.
18. Abbas S, Bashari M, Akhtar W, Li WW and Zhang X. 2014. Process optimization of ultrasound-assisted curcumin nanoemulsions stabilized by OSA-modified starch. *Ultrason. Sonochem*. **21**:1265-1274. https://doi.org/10.1016/j.ultsonch.2013.12.017.
19. Carpenter J, George S and Saharan VK. 2019. Curcumin encapsulation in multilayer oil-in-water emulsion: synthesis using ultrasonication and studies on stability and antioxidant and release activities. *Langmuir.* **35**:10866-10876. http://dx.doi.org/10.1021/acs.langmuir.9b01523.
20. Kean T and Thanou M. 2010. Biodegradation, biodistribution and toxicity of chitosan. *Adv. Drug Deliv. Rev*. **62**:3-11. https://doi.org/10.1016/j.addr.2009.09.004.
21. Shin GH, Chung SK, Kim JT, Joung HJ and Park HJ. 2013. Preparation of chitosan-coated nanoliposomes for improving the mucoadhesive property of curcumin using the ethanol injection method. *J. Agric. Food Chem*. **61**:11119-11126. https://doi.org/10.1021/jf4035404.
22. Stie MB, Gätke JR, Wan F, Chronakis IS, Jacobsen J and Nielsen HM. 2020. Swelling of mucoadhesive electrospun chitosan/polyethylene oxide nanofibers facilitates adhesion to the sublingual mucosa. *Carbohydr. Polym*. **242**:116428. https://doi.org/10.1016/j.carbpol.2020.116428.
23. Aditya N, Yang H, Kim S and Ko S. 2015. Fabrication of amorphous curcumin nanosuspensions using β-lactoglobulin to enhance solubility, stability, and bioavailability. *Colloids Surf. B*. **127**:114-121. https://doi.org/10.1016/j.colsurfb.2015.01.027.
24. Ahmed K, Li Y, McClements DJ and Xiao H. 2012. Nanoemulsion-and emulsion-based delivery systems for curcumin: Encapsulation and release properties. *Food Chem*. **132**:799-807. https://doi.org/10.1016/j.foodchem.2011.11.039.
25. Mun S, Decker EA and McClements DJ. 2006. Effect of molecular weight and degree of deacetylation of chitosan on the formation of oil-in-water emulsions stabilized by surfactant–chitosan membranes. *J. Colloid Interface Sci*. **296**:581-590. https://doi.org/10.1016/j.jcis.2005.09.023.
26. Chen X-G, Zheng L, Wang Z, Lee C-Y and Park H-J. 2002. Molecular affinity and permeability of different molecular weight chitosan membranes. *J. Agric. Food Chem*. **50**:5915-5918. https://doi.org/10.1021/jf020151g.
27. Koppolu B, Smith SG, Ravindranathan S, Jayanthi S, Kumar TKS and Zaharoff DA. 2014. Controlling chitosan-based encapsulation for protein and vaccine delivery. *Biomaterials.* **35**:4382-4389. https://doi.org/10.1016/j.biomaterials.2014.01.078.
28. Wei Z and Gao Y. 2016. Physicochemical properties of β-carotene bilayer emulsions coated by milk proteins and chitosan–EGCG conjugates. *Food Hydrocoll*. **52**:590-599. https://doi.org/10.1016/j.foodhyd.2015.08.002.
29. Chuah AM, Kuroiwa T, Kobayashi I and Nakajima M. 2009. Effect of chitosan on the stability and properties of modified lecithin stabilized oil-in-water monodisperse emulsion prepared by microchannel emulsification. *Food Hydrocoll*. **23**:600-610. https://doi.org/10.1016/j.foodhyd.2008.03.014.
30. Guan Y, Wu J and Zhong Q. 2016. Eugenol improves physical and chemical stabilities of nanoemulsions loaded with β-carotene. *Food Chem*. **194**:787-796. https://doi.org/10.1016/j.foodchem.2015.08.097.
31. Lee MH, Kim T-E, Jang HW, Chun YG and Kim B-K. 2021. Physical and turbidimetric properties of cholecalciferol-and men-

aquinone-loaded lipid nanocarriers emulsified with polysorbate 80 and soy lecithin. *Food Chem*. **348**:129099. https://doi.org/10.1016/j.foodchem.2021.129099.

32. Hosseini SMH, Gahruie HH, Razmjooie M, Sepeidnameh M, Rastehmanfard M, Tatar M, Naghibalhossaini F and Van der Meeren P. 2019. Effects of novel and conventional thermal treatments on the physicochemical properties of iron-loaded double emulsions. *Food Chem*. **270**:70-77. https://doi.org/10.1016/j.foodchem.2018.07.044.
33. Zhu Z, Wen Y, Yi J, Cao Y, Liu F and McClements DJ. 2019. Comparison of natural and synthetic surfactants at forming and stabilizing nanoemulsions: Tea saponin, Quillaja saponin, and Tween 80. *J. Colloid Interface Sci*. **536**:80-87. https://doi.org/10.1016/j.jcis.2018.10.024.
34. Masarudin MJ, Cutts SM, Evison BJ, Phillips DR and Pigram PJ. 2015. Factors determining the stability, size distribution, and cellular accumulation of small, monodisperse chitosan nanoparticles as candidate vectors for anticancer drug delivery: application to the passive encapsulation of [14C]-doxorubicin. *Nanotechnol Sci Appl*. 67-80. https://doi.org/10.2147/nsa.s91785.
35. Sari T, Mann B, Kumar R, Singh R, Sharma R, Bhardwaj M and Athira S. 2015. Preparation and characterization of nanoemulsion encapsulating curcumin. *Food Hydrocoll*. **43**:540-546. https://doi.org/10.1016/j.foodhyd.2014.07.011.